LUNAR IMPACT DEMAGNETIZATION: NEW CONSTRAINTS FROM MONTE CARLO MODELING AND MULTIPLE ALTITUDE MAGNETIC FIELD DATA.

Robert J. Lillis[1] (rlillis@ssl.Berkeley.edu), Jasper S. Halekas[1], Sarah T. Stewart[2], Karin L. Louzada[2,3], Michael E. Purucker[4], Michael Manga[5]

[1]UC Berkeley Space Sciences Laboratory, 7 Gauss Way, Berkeley, CA 94720

[2]Harvard University Department of Earth and Planetary Sciences, 20 Oxford St., Cambridge, MA 02138.

[3]Netherlands Office for Science & Technology, Netherlands Embassy, 4200 Linnean Ave NW, Washington, D.C.

[4]Planetary Geodynamics Laboratory, NASA Goddard Space Flight Center, Greenbelt, MD 20771

[5]UC Berkeley Department of Earth and Planetary Sciences, McCone Hall, Berkeley, CA 94720

Introduction: A substantial fraction of lunar impact craters >50 km in diameter show signs of shock demagnetization, with that fraction being larger for younger craters [1]. Though there are exceptions, in general for basins of Nectarian ages and younger, magnetic field at the surface increases between ~1 and ~4-5 transient cavity radii. Central positive magnetic anomalies, possibly indicative of thermoremanent magnetization of a central melt sheet, are quite prevalent for late pre-Nectarian and early Nectarian basins but are largely absent for late Nectarian, Imbrian, Eratosthenian, and Copernican-aged basins [2].

Shock demagnetization effects appear to extend out, in a monotonically decreasing fashion, to several crater radii in a monotonically decreasing fashion, implying that lunar magnetization has generally low coercivity and is partially demagnetized by shock pressures of less than 1 GPa [2]. In this work, we use statistical modeling of impact demagnetization signatures, along with radial magnetic field profiles at two different altitudes, in order to quantitatively constrain the average radius of impact demagnetization in addition to the lateral coherence wavelength and approximate bulk magnetization strength of the magnetization surrounding the basin. This technique has been successfully applied to Martian impact basins in a recently submitted paper [3].

Magnetic field: Data at 2 altitudes are taken from the Lunar Prospector mission: surface magnetic field magnitude estimates from electron reflectometry [4] ($B_{surface}$) and an internal lunar magnetic field model based on magnetometer measurements evaluated at 30 km altitude [5] ($B_{30\ km}$). Having multiple altitude data helps us to characterize the altitude decay of the magnetic field, and hence constrained quantities such as the coherence wavelength of the magnetization [3].

Fourier domain stochastic modeling of impact demagnetization signatures: To avoid the non-uniqueness inherent in inverse modeling of specific magnetic sources, we take a statistical approach and model the magnetic field observed over a cylindrically uniform demagnetized impact basin where the surrounding crustal magnetization is a random distribution filtered in Fourier space to have a Gaussian distribution in vertical and horizontal coherence scales and with an overall thickness of 20 km.. Figure 1 explains our methodology. We construct a large database of radial profiles of circumferential averages of magnetic field magnitude at 0 km and 30 km altitude for a range of different values of the following parameters:

1) strength, 2) direction, 3) vertical coherence wavelengthand 4) horizontal coherence wavelength of the surrounding magnetization plus 5) the demagnetization radius and 6) linear demagnetization gradient width.

Fitting results for lunar craters. These predicted circumferential averages are then compared/fitted to circumferentially-averaged radial profiles of both $B_{surface}$ and $B_{30\ km}$ for several lunar craters. The multiple altitudes allow useful constraints to be placed on the average magnetization strength, horizontal coherence wavelengthand demagnetization radius. Figure 2 demonstrates the fitting results for the Lower Imbrian-aged Schrödinger basin (which has a relatively clear demagnetization signature), making the assumption of 4 km vertical coherence wavelength. It shows that the mean radius of demagnetization is almost exactly equal to the main ring radius of 160 km, the best-fit horizontal coherence wavelength is ~120 km and that the mean bulk magnetization in the assumed 20 km-thick crust is around 0.01 A/m. We intend to extend this analysis to other demagnetized lunar craters.

Conclusions: The radius of shock-induced demagnetization [3] can be combined with pressure-demagnetization curves for lunar magnetic carriers [6] and peak pressure contours from families of lunar impact simulations [7, 8] to help constrain the impact energyfor specific lunar basins The coherence scale of magnetization in the crust will inform the formation processes and evolution of lunar crustal magnetism.

References: [1] Halekas, J.S. et al., *GRL*, 29, 1645, 2002, [2] Halekas, J.S. et al., *MAPS*, 38, 4 565-578, 2003, [3] Lillis, R. J. et al., submitted to *JGR*, 2010, [4] Halekas, J. S. et al. *JGR, 106,* 27,841-52, 2001, [5] Purucker, M. E., 2008, *Icarus, 197,* 19-23. [6] Louzada, K. L. et al., *EPSL* (submitted), 2010, [7] Louzada, K.L. and Stewart, S.T., *GRL*, *36*, L15203, 2009 [8] Stewart, S. T. et al., LPSC 2010.

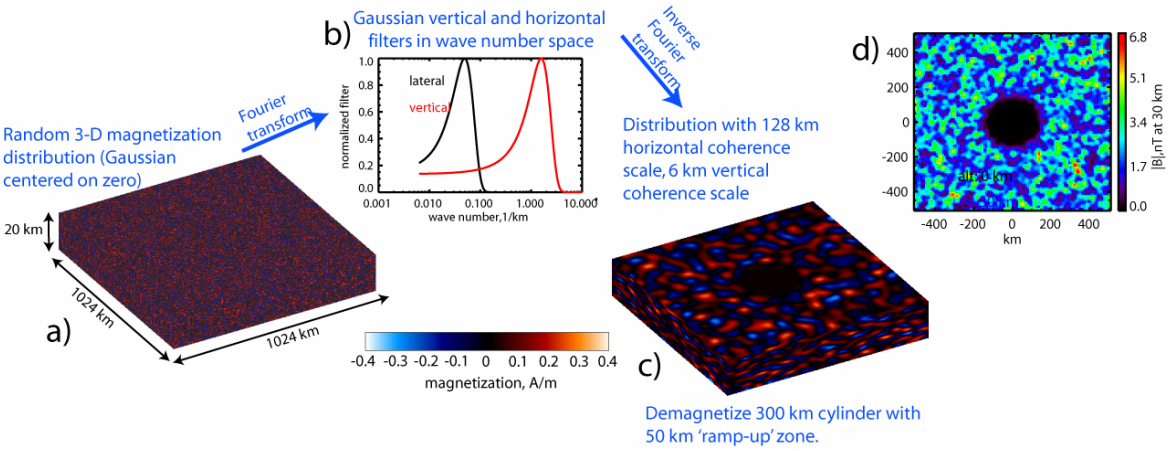

Figure 1: Statistical Fourier domain modeling. A) A 48 x 256 x 256-element random magnetization distribution where each voxel's value is drawn from a zero-centered Gaussian distribution with a standard deviation of 0.1 A/m. b) Gaussian horizontal and vertical filters of 128 km and 4 km in the wave number domain. c) The inverse Fourier transform of the filtered wave number domain distribution with a 300 km-diameter cylinder of zero magnetization, with a uniform 50 km-wide radial 'ramp-up' zone. d) The resulting magnetic field magnitude measured at 30 km altitude above the distribution shown in panel c.

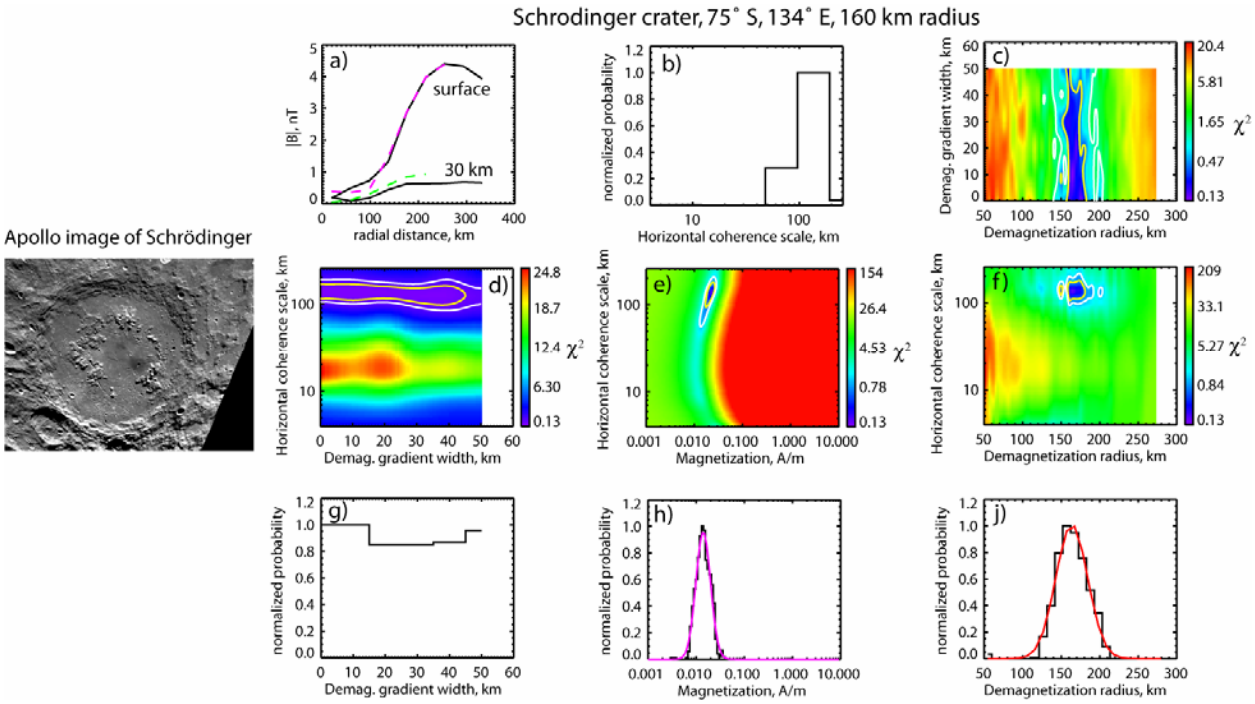

Figure 2: Crustal demagnetization and impact demagnetization fitted parameters for Schrödinger crater. a) Radial profiles of circumferentially averaged magnetic field at the surface and 30 km altitude, over which the best-fit model predictions are plotted with pink and green dashed lines respectively. b) Histogram of the distribution of values of horizontal coherence wavelength within the 1-sigma confidence interval. Panels c) through j) are arranged symmetrically, with demagnetization gradient width as the abscissa in the left column, magnetization strength in the middle column and demagnetization radius in the right column and horizontal coherence wavelength as the ordinate in the middle row. c) through f) Four different two-dimensional slices of the 4-dimensional χ^2 space defined by demagnetization radius, demagnetization gradient width, magnetization strength and horizontal coherence wavelength. Each 2-d slice correspondents to the χ^2 minimum in the other two dimensions. The white contour corresponds to the 1-sigma confidence interval.